PERFORMANCE ANALYSIS FOR PLATE HEAT EXCHANGER WITH VARIOUS CHEVRON ANGLES USING R134A AS A REFRIGERANT

Amala Justus Selvam. M,

Professor, Automobile Department,
Vel Tech Dr Rr & Dr SR Technical University,
Chennai, India.

Velu. R,

Asso. Prof, Mechanical Department,Vel Tech
Dr Rr & Dr SR Technical University,
Chennai, India.

ABSTRACT

Analysis to measure the condensation heat transfer coefficient and the pressure drop in brazed plate heat exchangers (BPHEs) were conducted with the refrigerants R134a. Brazed plate heat exchangers with different chevron angles of 45°, 35°, and 20° were used. Changing the mass flux, the condensation temperature, and the vapour quality of the refrigerant, the condensation heat transfer coefficient and the pressure drops were measured. Both the heat transfer coefficient and the pressure drop increased proportionally with the mass flux and the vapour quality and inversely with the condensation temperature and the chevron angle. Correlations of the Nusselt number and the friction factor with the geometric parameters are suggested for the tested BPHEs.

Keywords: Condensation, Brazed plate heat exchanger, R134a, Chevron angle.

INTRODUCTION:

Plate heat exchangers (PHEs) were introduced in the 1930s and were almost exclusively used as liquid/liquid heat exchangers in the food industries because of their ease of cleaning. Over the years, the development of the PHE has generally continued towards larger capacity, as well as higher working temperature and pressure. Recently, a gasket sealing was replaced by a brazed material, and each thermal plate was formed with a series of corrugations (herringbone or chevron). These greatly increased the pressure and the temperature capabilities. The corrugated pattern on the thermal plate induces a highly turbulent fluid flow. The high turbulence in the PHE leads to an enhanced heat transfer, to a low fouling rate, and to a reduced heat transfer area. Therefore, PHEs can be used as alternatives to shell-and-tube heat exchangers. Due to ozone depletion, the refrigerant R22 is being replaced by R134a (a binary mixture of R32 and R125, mass fraction 50 %/50 %). R134a approximates an azeotropic behaviour since it can be regarded as a pure substance because of the negligible temperature gliding. The heat transfer and the pressure drop characteristics in PHEs are related to the hydraulic diameter, the increased heat transfer area, the number of the flow channels, and the profile of the corrugation waviness, such as the inclination angle, the corrugation amplitude, and the corrugation wavelength. These geometric factors influence the separation, the boundary layer, and the vortex or swirl flow generation. However, earlier experimental and numerical works were restricted to a single-phase flow. Since the advent of a Brazed PHE (BPHE) in the 1990s, studies of the condensation and/or evaporation heat transfer have focused on their applications in refrigerating and air conditioning systems, but only a few studies have been done. Much work is needed to understand the features of the two-phase flow in the BPHEs with alternative refrigerants. Xiaoyang et al. [1] experimented with the two-phase flow distribution in stacked PHEs at both vertical upward and downward flow orientations. They indicated that non-uniform distributions were found and that the flow distribution was strongly affected by the total inlet flow rate, the vapour quality, the flow channel orientation, and the geometry of the inlet port.

Holger [2] theoretically predicted the performance of chevron-type PHEs under single-phase conditions and recommended the correlations for the friction factors and heat transfer coefficients as functions of the corrugation chevron angles. Lee et al. [3] investigated the characteristics of the evaporation heat transfer and pressure drop in BPHEs with R404A and R407C. Kedzierski [4] reported the effect of inclination on the performance of a BPHE using R22 in both the condenser and the evaporator. Several single-phase correlations for heat transfer coefficients and friction factors have been proposed, but few correlations for the two-phase flow have been proposed. Yan et al. [5] suggested a correlation of condensation with a chevron angle of 30° for R134a. Yan et al. reported that the mass flux, the vapour quality, and the condensation pressure affected the heat transfer coefficients and the pressure drops. Hieh and Lin [6] developed the correlations for evaporation with a chevron angle of 30° for R134a.

EXPERIMENTAL FACILITY:

In The experimental facility is capable of determining in plate heat transfer coefficients and measuring the pressure drops for the refrigerants. It consists of four main parts: a test section, a refrigerant loop, two water loops, and a data-acquisition system. A schematic of the test facility used in this study is shown in Fig. 1, and detailed descriptions of the four main parts are mentioned below.
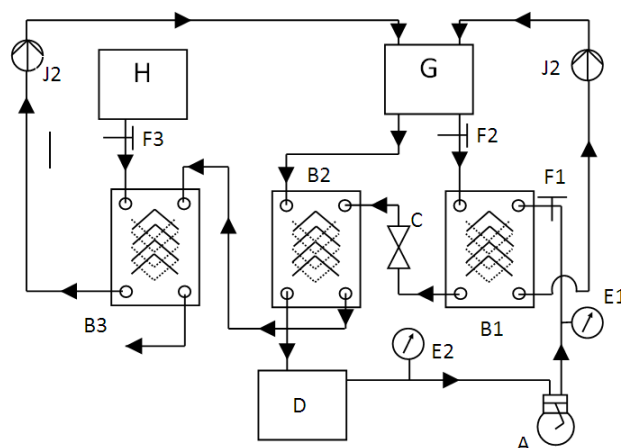

Fig.1 Schematic diagram of the Experimental setup

A. Compressor,   B1, B2 and B3. PHE, C. Expansion Valve, D. Heater,   E1 and E2. Pressure Gauge, F1, F2 and F3. Regulator, G. Milk Tank, H. Water Tank   J1 and J2. Pump.

BRAZED PLATE HEAT EXCHANGER:

Three BPHEs with chevron angles of 45°, 35°, and 20° were used as the test sections. The angles of corrugation were measured from the horizontal axis. Each BPHE was composed of 4 thermal plates and 2 end plates, forming 5 flow channels. The dimensions of the BPHEs are shown in Fig. 2. The refrigerant and cooling water were directed into the alternate passages between the plates through corner ports, creating counter flow conditions. The cooling water owed from the bottom to the top of every other channel on the basis of a central channel. On the other hand, the refrigerant owed from the top to the bottom in the rest of them.

REFRIGERANT LOOP:

Refrigerant was supplied to the test section at specific conditions (i.e., temperature, flow rate, and quality) through the refrigerant loop. This loop contained a pre-heater, a double-pipe heat exchanger, a receiver, a magnetic gear pump, a differential pressure transducer, and a mass flow meter. Also included were thermocouples probes and pressure taps at the inlet/outlet of the test section. The refrigerant pump was driven by a DC motor which was controlled by a variable DC output motor controller.

The refrigerant flow rate was measured by using a mass flow meter installed between the magnetic gear pump and the pre-heater with an accuracy of 0.5 %. The pre-heater located before the test section was used to evaporate the refrigerant to a specified vapour quality at the inlet of the test section. The pressure drop of the refrigerant owing through the test section was measured with the differential pressure transducer, to an accuracy of 0.25 kPa. The refrigerant through the test section was sub-cooled at a double-pipe heat exchanger by the water cooled by the chiller and went into a liquid receiver. The sub-cooled refrigerant returned to the magnetic gear pump and circulated through the refrigerant loop repeatedly. Calibrated T-type thermocouples were used to measure the temperatures of the refrigerant at the inlet/outlet of the test section. The entire loop was insulated with fibre glass to prevent heat transfer to the environment.
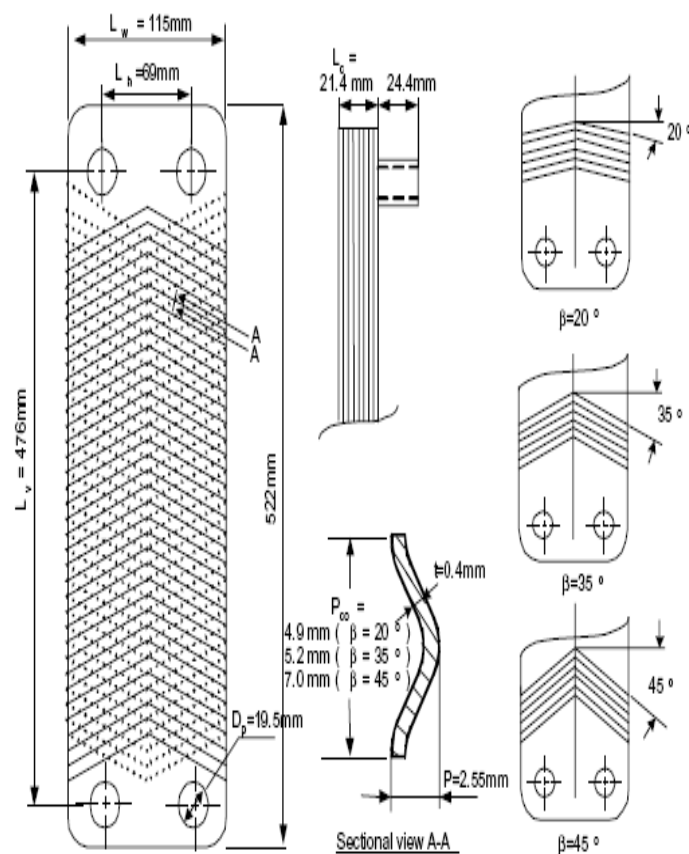

Fig. 2 Dimensions of BPHE.

WATER LOOP:

There are two closed water loops in this facility. One is for determining the condensation heat flux at the test section. The other is for making the sub-cooled refrigerant state at two double-pipe heat exchangers before it enters the magnetic gear pump. The water flow rates of the test section were measured by using a turbine flow meter, and T-type thermocouples were installed to evaluate the gain of the heat flux of the water of the test section.

DATA ACQUISITION:

The data were recorded by a computer-controlled data-acquisition system with 40 channels scanned at the speed of 30 data per minute. The temperature and the pressure of both fluids were continuously recorded, and the thermodynamic properties of the refrigerant were obtained from a computer program. After steady-state conditions had been reached in the system, all measurements were taken for 10 minutes.

DATA REDUCTION AND UNCERTAINTY ANALYSIS:

The hydraulic diameter of the channel, D_h, is defined as

$$D_h = \frac{4 \times \text{channel flow area}}{\text{wetted perimeter}} = \frac{4bL_w}{2L_w\phi} = \frac{2b}{\phi}, \qquad (1)$$

The mean channel spacing, b, is defined as

$$b = p - t; \qquad (2)$$

and the plate pitch p can be determined as

$$p = \frac{L_c}{N_t - 1}. \qquad (3)$$

The procedures to calculate the condensation heat transfer coefficient of the refrigerant side are described below. At first, the refrigerant quality at the inlet of the test section (x_{in}) should be selected to evaluate the condensation heat at a given quality. Its value is calculated from the amount of heat given by a pre-heater, which is the summation of the sensible heat and the latent heat:

$$Q_{pre} = Q_{sens} + Q_{lat} \qquad (4)$$

The refrigerant quality at the inlet of the test section can be written as

$$x_{in} = \frac{1}{i_{fg}} \left[\frac{Q_{pre}}{\dot{m}_r} - C_{p,r}(T_{r,sat} - T_{r,pre,in}) \right]. \qquad (5)$$

The power gained by the pre-heater is calculated by measuring the voltage and the current with a power meter. The change in the refrigerant quality inside the test section was evaluated from the heat transferred in the test section and the refrigerant mass flow rate:

$$\Delta x = x_{in} - x_{out} = \frac{Q_w}{\dot{m}_r \times i_{fg}}. \qquad (6)$$

The condensing heat in the test section was calculated from an energy balance with water:

$$Q_w = m_w Cp_w(T_{w;out} - T_{w;in}) \qquad (7)$$

The heat transfer coefficient of the refrigerant side (h_r) was evaluated from the suitable equation. The overall heat transfer coefficient was determined using the log mean temperature difference formula.The heat transfer coefficient of the water side (h_w) was obtained using the equation that was developed from the single-phase water to water pre-tests by Kim [7]. If the least-squares method and the multiple regression method are used, the heat transfer coefficient of the water side is correlated in terms of the Reynolds number, the Prandtl number, and the chevron angle. The thermal resistance of the wall is negligible compared to the effect of convection. For the vertical downward flow, the total pressure drop in the test section is defined as

$$P_{total} = P_{fr} + P_a + P_s + P_p; \qquad (8)$$

and P_{total} is measured by using a differential pressure transducer.

The port pressure loss in this experiment was less than 1 % of the total pressure loss. The static head loss can be written as and it has a negative value for vertical downward flow. The acceleration pressure drop for condensation is expressed as

$$\Delta P_p = 1.4 G_p^2/(2\rho_m),$$

Where

$$G_p = 4\dot{m}_{Eq}/\pi D_p^2 \qquad\qquad 10$$

and

$$(1/\rho_m) = (x/\rho_g) + [(1-x)/\rho_f]. \qquad 11$$

An uncertainty analysis was done for all the measured data and the calculated quantities based on the methods described by Moffat [9]. The detailed results of the uncertainty analysis are shown in Table 1.

Table I: Estimated Uncertainty

Parameters	Uncertainty
Temperature	$\pm 0.2^{o}C$
Pressure	$\pm 4.7kPa$
Pressure drop	$\pm 250Pa$
Water flow rate	$\pm 2\%$
Refrigerant mass flux	$\pm 0.5\%$
Heat flux of test section	$\pm 5.7\%$
Vapour quality	± 0.03
Heat transfer coefficient of water side	$\pm 10.1\%$
Heat transfer coefficient of refrigerant side	$\pm 9.1\%$

The equivalent mass flow rate, m_{Eq} is defined as

$$\dot{m}_{Eq} = \dot{m}\left[1 - x + x\left(\frac{\rho_f}{\rho_g}\right)^{0.5}\right]. \qquad\qquad 12$$

The port Pressure loss in this experiment was less than 1% of the total pressure loss. The static loss can be written as

$$\Delta P_s = -\rho_m g L_v \qquad\qquad 13$$

and it has a negative value for vertical downward flow. The acceleration pressure drop for condensation is expressed as

$$\Delta P_a = -\left[(G_{Eq}^2 x/\rho_{fg})_{in} - (G_{Eq}^2 x/\rho_{fg})_{out}\right] \qquad 14$$

RESULTS AND DISCUSSION:

The condensation heat transfer coefficients and the pressure drops of R134a were measured in three BPHEs with chevron angles of 20, 35, and 45 degrees by varying the mass flux (13 to 34 kg/m2s), the vapour quality (0.9 to 0.15), and the condensing temperature (20oC and 30oC) under a given heat flux condition (4.7 to 5.3 kW/m2).

FLOW REGIME:

Before the behaviours of heat transfer are considered, it is necessary to predict what flow regime exists at a given set of operating conditions. The detailed flow regime map for the PHE has not been proposed yet because of the difficulty of flow visualization. Vlasogiannis et al. [10] suggested the criterion of a two-phase flow regime for a PHE in terms of superficial liquid (j_f) and vapour velocities (j_g) by using water and air under adiabatic conditions. They only simulated a mixture of water and air as a two-phase fluid. According to their work, the flow patterns in a PHE are significantly different from those inside the vertical round tubes. They detected 3 types of flow patterns. The first was a gas continuous pattern with a liquid pocket at flow water flow rates (jf < 0.025 m/s) over wide range of air flow rates. The second was the slug flow pattern, which was detected at sufficiently high air (jg > 2 m/s) and water flow rates (jf > 0.025 m/s). Thirdly, the liquid continuous pattern with a gas pocket or a gas bubble at the high water flow rates (jf >0.1 m/s) and low air flow rates (jg < 1 m/s).According to the flow regime map proposed by Vlasogiannis et al., the expected flow pattern in this experimental study is the gas continuous flow pattern with liquid pockets. However, their flow regime map has a significant limitation for use since many important features, such as the phase-change, the heating or cooling

conditions, the densities or specific volumes of the working fluids, the geometries of the PHEs, etc., were not considered in detail. According to the flow regime map proposed by Crawford et al. [11], which was developed for vertical downward flow in a round tube, all experimental flow patterns are located in the intermittent flow regime, but this flow regime cannot represent the correct flow regime in a BPHE due to the different geometries.

CONDENSATION HEAT TRANSFER:

Figure 3 and 4 shows the effects of the refrigerant mass flux, the chevron angle, and the condensation temperature on the averaged heat transfer coefficient for R134a. The term `averaged heat transfer coefficient' means the average of the heat transfer coefficients calculated by varying the quality of the refrigerant from 0.15 to 0.9, and the coefficients were obtained from Eq. (15):

$$h_{averged} = \frac{\sum h_{local} x_{local}}{\sum x_{local}} \qquad 15$$

where h_{local} is the local heat transfer coefficient at the local vapour quality. The experimental results indicate that the averaged heat transfer coefficients vary proportionally with the mass flux and inversely with the chevron angles and the condensation temperature.

The small chevron angle forms narrow pitches to the flow direction, creating more abrupt changes in the velocity and the flow direction, thus increasing the effective contact length and time in a BHPE. The zigzag flow increases the heat transfer, and the turbulence created by the shape of the plate pattern is also important in addition to the turbulence created by the high flow rates. Increasing the mass flux at a given condensation temperature showed that the differences in the averaged heat transfer coefficients were significantly enlarged with decreasing chevron angle. This indicates that a PHE with the small chevron angle is more effective at a large mass flux (Gc > 25 kg/m2s) than at a small mass flux.

The averaged heat transfer coefficient of R134a decreases with increasing condensation temperature. The vapour velocity is a more influential factor than the liquid film thickness for the heat transfer. Vapour bubbles in the flow enhance the disturbance in the bubble wake as a turbulence promoter, and the turbulence induced by the vapour bubbles increases with the vapour velocity. Also, since the specific volume of the vapour increases with decreasing condensation temperature, the vapour velocity increases for a fixed mass flux and quality.
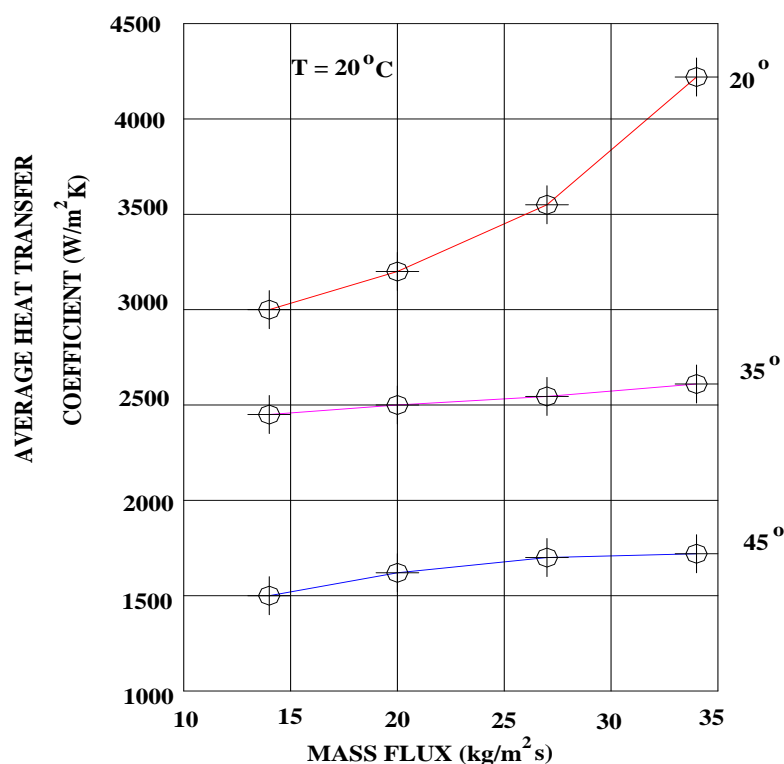

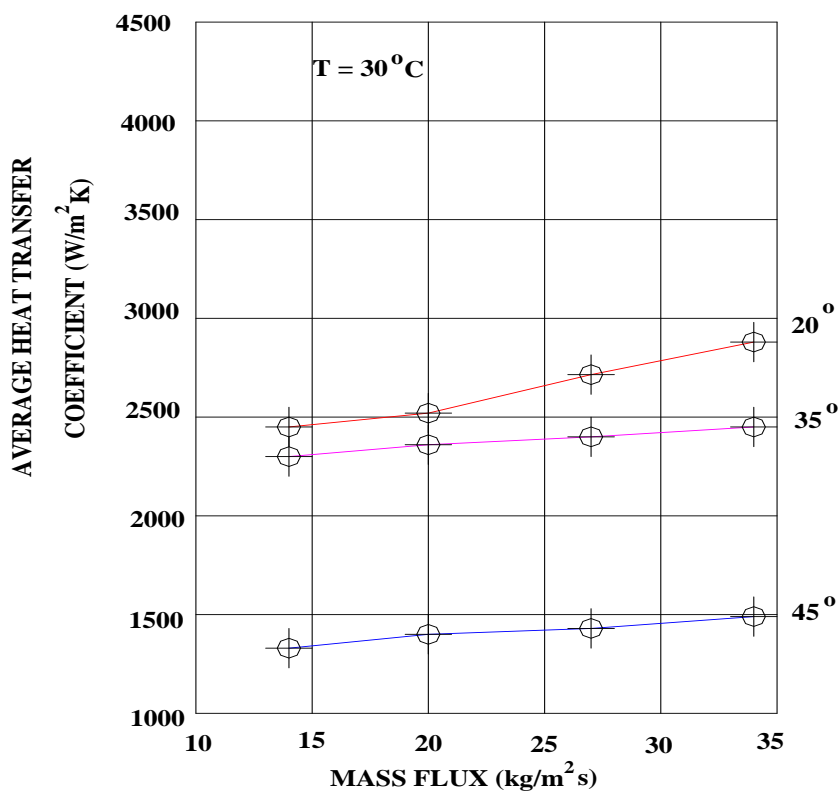**Fig. 3 Effect of mass flux on the averaged heat transfer coefficient (T = 20°C)**

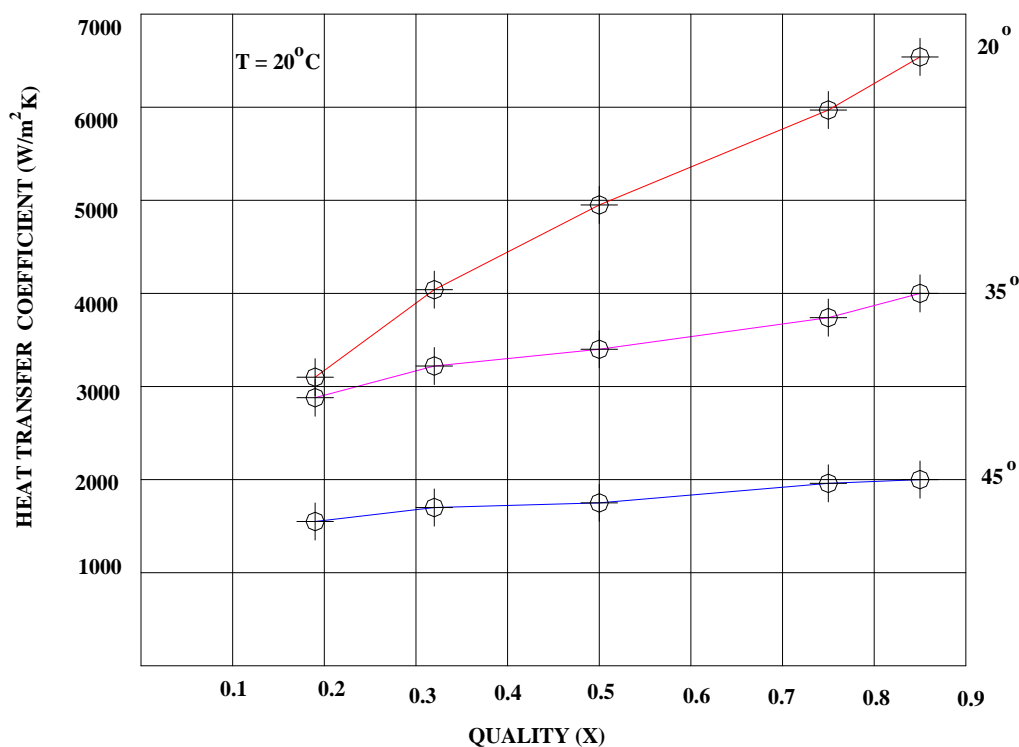**Fig. 4 Effect of mass flux on the averaged heat transfer coefficient (T = 30°C)**

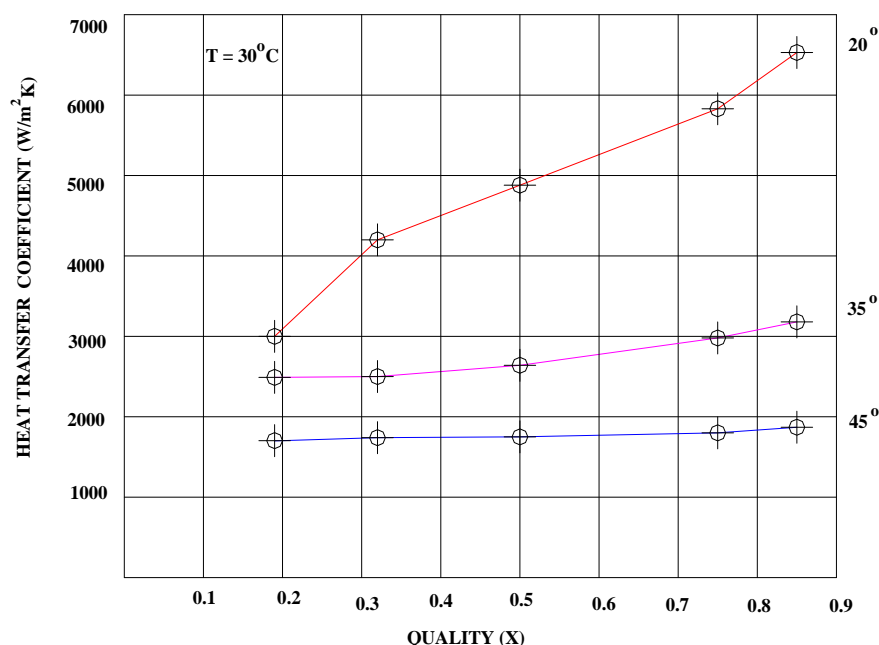**Fig.5 Effect of quality on the heat transfer coefficient (T= 20°C)**

Fig. 6 Effect of quality on the heat transfer coefficient (T= 30°C)

The vapor velocity at 20°C is faster than that at 30°C. The rates of the averaged heat transfer coefficients between condensation temperatures of 20°C and 30°C increased 5 % for a chevron angle of 45°, 9 % for 35°, and 16 % for 20°. These results show that different chevron angles lead partly to different flow pattern. Thus, we may conclude that the flow regime map should be modified by geometric considerations. The heat transfer coefficients in the high-quality region (fast velocity region) are larger than those in the low-quality region (slow velocity region). As mentioned above, this happens because the vapour velocity is the dominant effect on the heat transfer mechanism. Increasing the vapour quality at the same mass flux induces a faster bubble velocity, which increases the turbulence level and the convection heat transfer coefficient. The difference of heat transfer coefficients between the low-quality region and the high-quality region becomes larger with decreasing chevron angle. The PHE with a low chevron angle shows a better heat transfer performance in the high-quality region (i.e., the high vapour velocity region). Fig. 5 also shows the variation of the heat transfer coefficients with the condensation temperatures. Like Fig. 6, the heat transfer coefficients decreased with increasing condensation temperature. Also, the variations of the heat transfer coefficients with the condensation temperature are larger in the high-quality region. From the experimental results in Figs. 5 and 6, lowering the chevron angle and the condensation temperature gives the desired heat transfer effect. The ratio of the cost of the BCE test setup to the cost of the double cup extrusion test setup, for conducting the experiments on same sizes of billets works out to 1:3. As such BCE test is simpler and cheaper compared to DCE test to conduct and to obtain good results without sacrificing the accuracy.

FRICTIONAL PRESSURE LOSS:

The frictional pressure loss in a BPHE is obtained by subtracting the acceleration pressure loss, the static head loss, and the port pressure loss from the total pressure loss. Figure 7 shows the trend of the pressure drop along the mass flux, and Fig. 8 shows the trend of the pressure drop along the mass flux (30°C) at a mass flux of 34 kg/m^{2}s and a heat flux of 4.7 to 5.3 kW/m^2. The frictional pressure drops in the BPHEs increase with increasing mass flux and quality and decreasing condensation temperature and chevron angle. This trend is similar to that of the condensation heat transfer. As mentioned above, since the vapour velocity is much faster than the liquid velocity during the two-phase flow in the tube, the vapour velocity is the dominant influence on the pressure drop, as well as the heat transfer. A high vapour velocity also tends to increase the turbulence of the flow. From Figs. 3, 4, 5 , 6, 7 and 8 we may concluded that since the trends of the condensation heat transfer and the pressure loss in BPHEs are similar, those effects must be carefully considered in the design of a BPHE.
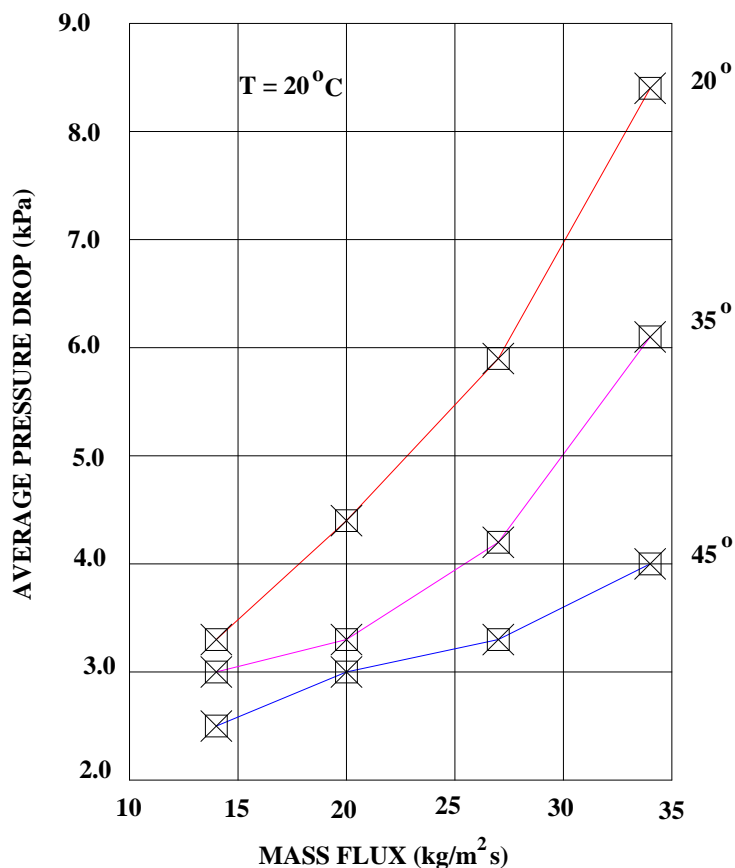
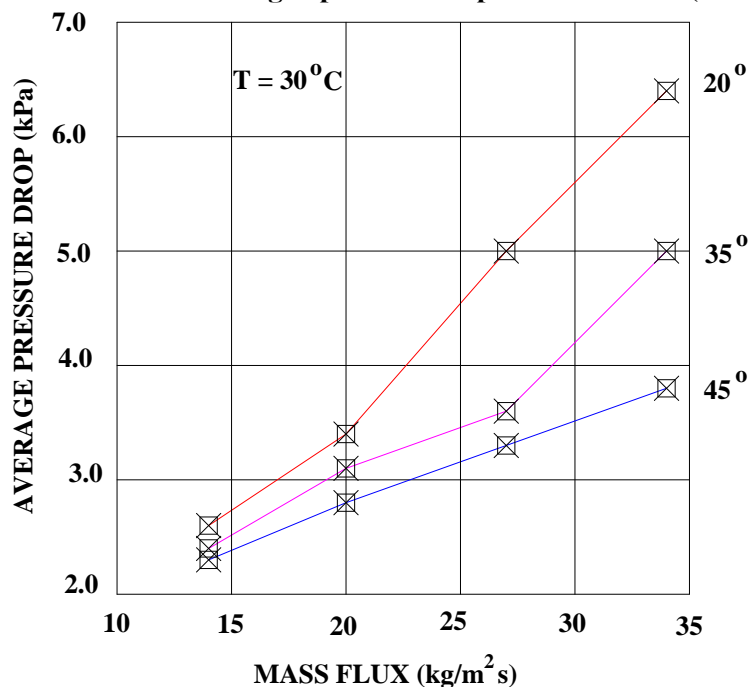**Fig. 7 Variation of the averaged pressure drop with mass flux (T= 20°C)**

Fig. 8 Variation of the averaged pressure drop with mass flux (T= 30°C)

CORRELATION OF NUSSELT'S NUMBER:

Based on the experimental data, the following correlations for Nu and f during condensation for the tested BPHEs are established

$$Nu = Ge_1 Re_{Eq}^{Ge_1} Pr^{1/3}, \qquad\qquad 16$$

$$Ge_1 = 11.22 \left(\frac{p_{co}}{D_h}\right)^{-2.83} \left(\frac{\pi}{2} - \beta\right)^{-4.5}, \qquad 17$$

$$Ge_2 = 0.35 \left(\frac{p_{co}}{D_h}\right)^{0.23} \left(\frac{\pi}{2} - \beta\right)^{1.48}, \qquad 18$$

$$f = Ge_3 Re_{Eq}^{Ge_4},$$

$$Ge_3 = 3521.1 \left(\frac{p_{co}}{D_h}\right)^{4.17} \left(\frac{\pi}{2} - \beta\right)^{-7.75}, \qquad 19$$

$$Ge_4 = -1.024 \left(\frac{p_{co}}{D_h}\right)^{0.0925} \left(\frac{\pi}{2} - \beta\right)^{-1.3} \qquad 20$$

where Ge1, Ge2, Ge3, and Ge4 are non-dimensional geometric parameters that involve the corrugation pitch, the equivalent diameter, and the chevron angle. ReEq is the equivalent Reynolds number, and GEq the equivalent mass flux: where Gc is the channel mass flux. The suggested correlations for the Nusselt number and the friction factor can be applied in the range of ReEq from 300 to 4000. The correlation of Yan et al. is

$$Re_{Eq} = \frac{G_{Eq} D_h}{\mu_f},$$

$$G_{Eq} = G_c [1 - x + x(\rho_f/\rho_g)^{1/2}] \qquad 22$$

$$G_c = \frac{\dot{m}}{N_{cp} b L_w}, \qquad 23$$

and is obtained from one PHE with a chevron angle of 30° for R134a. Regardless of the BPHE types and refrigerants, most of the experimental data are within 20 % for the correlation proposed in this paper. The correlation of Yan et al. matched the data relatively well for 20° and 35° within 30 %, but over-predicted the data quite a bit for 45°. Because a BPHE has a strong geometric effect, the correlation with geometric parameters must be developed for general applications. Similar to the correlation of the Nusselt number, the correlation of the friction factor includes the equivalent Reynolds number and the geometric parameters. Regardless of the BPHE types and refrigerants, most of the experimental data are within 15 % of the correlation proposed in this paper; the r.m.s. deviation for Eq. (22) is 10 %.

CONCLUSIONS:

An experimental investigation has been carried out to measure the condensation heat transfer coefficient and the pressure drop of R134a in BPHEs with chevron angles of 20°, 35°, and 45°. The CFD data were taken at two condensation temperatures of 20°C and 30°C in the range of mass flux of 14-34 kg/m^2 s with a heat flux of 4.7 - 5.3 kW/m^2.

Both the heat transfer coefficient and the pressure drop increased proportionally with the mass flux and the vapour quality and inversely with the condensation temperature and the chevron angle. These effects must be carefully considered in the design of a BPHE due their opposing effects.

Correlations for the Nusselt number and the friction factor with the geometric parameters were put forth for the tested BPHEs within 20 % (r.m.s. deviation: 10.9 %) for Nu and 15 % (r.m.s. deviation: 10 %) for f.

REFERENCES:

[1] R. Xiaoyang, K. Masahiro and J. G. Burgers,(1995), *ASME 225, 115.*
[2] M. Holger, (1996), *Chem. Eng. Proc. 35, 301.*
[3] G. J. Lee, J. Lee, C. D. Jeon and O. K. Kwon, (1999), *Proceedings of the 1999 Summer Meeting of the SAREK*, pp.144.
[4] M. A. Kedzierski, (1997), *Heat Trans. Eng.* pp.18-25.
[5] Y. Y. Yan, H. C. Lio and T. F. Lin, (1999), *Int. J. Heat and Mass Transfer Vol.42*, pp. 993.
[6] Y. Y. Hsieh and T. F. Lin, (2002), *Int. J. Heat and Mass Transfer 45*, pp.1033.
[7] Y. S. Kim, (1999), *M.S. Thesis*, Yonsei University.
[8] S. Kakac and H. Liu, (1998), Heat Exchangers Selection, Rating and Thermal Design, pp.323.
[9] P. Vlasogiannis, G. Karajiannis and P. Argyoropoulos, (2002), *Int. J. Multiphase Flow, Vol.28*, pp.757.
[10] T. J. Crawford, C. B. Weinberger and J. Weisman, (1985), *Int. J. Multiphase Flow Vol.11*, pp.297.